



Magnetization Studied as a Function of Temperature and Magnetic Field for Ferromagnetic Transition in DMNaFe

E. KILIT DOGAN^{1,4} and H. YURTSEVEN^{2,3,5}

1.—Department of Physics, Van Yuzuncu Yil University, 65080 Van, Turkey. 2.—Physics Group, Middle East Technical University, Northern Cyprus Campus, Kalkanli via Mersin 10, Guzelyurt, Turkey. 3.—Department of Physics, Middle East Technical University, 06531 Ankara, Turkey. 4.—e-mail: ekilit@yyu.edu.tr. 5.—e-mail: hamit@metu.edu.tr

Magnetization has been calculated as a function of temperature in the ferromagnetic phase of $(\text{CH}_3)_2\text{NH}_2\text{Na}_{0.5}\text{Fe}_{0.5}(\text{HCOO})_3$ denoted by DMNaFe as one of the metal formate framework by using molecular field theory. Calculated $M(T)$ is compared with the magnetization measured as a function of temperature ($H = 10$ Oe) in field-cooling and zero-field-cooling regimes from the literature, and a power-law analysis of the experimental data was performed for DMNaFe. Magnetization measured as a function of the magnetic field, as reported in the literature, has also been analyzed by the power-law formula. The magnetization indicates a weak first-order (or nearly second-order) ferromagnetic transition in DMNaFe.

Key words: Ferromagnetic transition, magnetization, DMNaFe

INTRODUCTION

Hybrid organic–inorganic materials, in particular, metal–organic frameworks (MOFs), have been studied extensively because of their various structures which can be changed by using different organic ligands and metal ions.^{1–4} MOFs have potential applications as catalysts, chemical sensors, and luminescent materials,^{2,5,6} which are attractive for gas storage,^{7–9} and they possess good gas sorption and luminescence properties,^{10,11} as previously indicated.^{12,13}

MOFs are the multiferroic materials which exhibit two coexisting orders among the electric and magnetic (also elastic). Thus, as mainly oxides of transition metal elements,¹⁴ they are widely used for dynamic random access memories, data storage media, telecommunication systems, and electromagnetic sensors, etc.,^{15,16} as also stated in an earlier study.¹⁷ As multiferroic materials, they undergo order–disorder transition, and also some perovskite MOFs, such as a heterometallic $(\text{CH}_3)_2\text{NH}_2\text{Na}_{0.5}\text{Fe}_{0.5}(\text{HCOO})_3$ or shortly DMNaFe, exhibit

structural phase transition^{12,13} with the $R\bar{3}$ symmetry at 293 K and the triclinic symmetry at 110 K.¹² This compound undergoes a magnetic phase transition at $T_m = 8.5$ K with a small hysteresis in the magnetization $M(H)$, as measured, indicating a ferromagnetic character of the ordering.¹² It exhibits a weak ferromagnetism due to a small canting of the underlying antiferromagnetic lattice.¹² It has been pointed out¹² that the small saturation magnetization of DMNaFe, as in the other metal formates templated by dimethylammonium,^{17–20} ammonium,²¹ and imidazolium,²² is consistent with the spin-canted mechanism of the long-range magnetic ordering in DMNaFe. Magnetization of DMNaFe has been measured in a nominal magnetic field of 10 Oe under zero-field cooling (ZFC) and field-cooling (FC) conditions.¹² Recently, we have calculated the magnetization of DMMn and chromium-doped DMMn,²³ magnetization, magnetic susceptibility and the specific heat in heterometallics.²⁴ In addition, we have investigated the magnetic ordering of the two mixed-valence iron (II)–iron (III) metal formate framework (MOFs).²⁵

In this study, we perform a power-law analysis of the magnetization, $M(T)$, as a function of temperature by using the experimental data in the ZFC and FC regimes at 10 Oe,¹² and we deduce the values of

(Received April 10, 2020; accepted August 1, 2020)

the critical exponent, β , for the order parameter (magnetization) below $T_c = 8.5$ K for DMNaFe. Our second analysis is the field dependence of the magnetization, $M(H)$, through the power-law formula by using the experimental data.¹² From this analysis, we extract the values of the critical isotherm, δ (at $T = T_c$), for DMNaFe. In the second part of this study, we calculate the temperature-dependence of the magnetization, $M(T)$, in the ZFC and FC regimes by means of molecular field theory (MFT)^{26,27} for DMNaFe. Calculated $M(T)$ is compared with the experimental data¹² for this compound.

In ‘‘Theory’’ section we introduce an outline of the theory. In ‘‘Calculations and results’’ section, calculations and results are given. Sections ‘‘Discussion and Conclusions’’ give our discussion and conclusions, respectively.

THEORY

In order to investigate the magnetic properties of MOFs which undergo order–disorder transitions, we employ here two theoretical models, namely, the Ising and Heisenberg models. On the basis of the classic Weiss theory of ferromagnetism, the Hamiltonian of the Heisenberg and Ising models under the field can be described as:

$$H = -\frac{1}{2} \sum v_{ij} \vec{S}_I \vec{S}_j - \mathcal{H} \sum \vec{S}_I \text{ Heisenberg} \quad (1a)$$

and:

$$H = -\frac{1}{2} \sum v_{ij} \mu_I \mu_j - \mathcal{H} \sum \mu_I \text{ Ising} \quad (1b)$$

respectively, where v_{ij} is the exchange force between spins I and j , \vec{S}_I is the spin operator of the spin at site I (Heisenberg model), μ_I is the z component of spin $\frac{1}{2}$ which can take values of ± 1 (Ising model) and \mathcal{H} is the external field (in the units of energy), as given by Brout.²⁶ Spins in the Heisenberg model are isotropically coupled, whereas in the Ising model the coupling is completely anisotropic as a classical model since all operators μ_I commute.²⁶

For crystalline structures, Yamada et al.²⁸ has developed an Ising pseudospin–phonon coupled model by considering the NH_4Br crystal according to the Hamiltonian:

$$H = \frac{1}{2} \left(\sum_{\vec{k}s} p_{\vec{k}s} p_{\vec{k}s}^* + w_{\vec{k}s}^2 q_{\vec{k}s} q_{\vec{k}s}^* \right) - \frac{1}{2} \sum_{ij} J_{ij} \sigma_i \sigma_j - \sum_{\vec{k}s} \sum_I \frac{w_{\vec{k}s}}{\sqrt{N}} g_{\vec{k}s} q_{\vec{k}s} \sigma_I e^{i\vec{k} \cdot \vec{r}_i} \quad (2)$$

where $p_{\vec{k}s}$ and $q_{\vec{k}s}$ denote the momentum and the coordinate of the phonon with the wave vector \vec{k} and mode s , respectively, and $w_{\vec{k}s}$ is the characteristic frequency of the phonon. σ_i and σ_j represent the spin

variables as μ_i and J_{ij} is the interaction parameter as v_{ij} in the Ising model (Eq. 1b). In Eq. 2, the first term describes the phonon energy, the second term with the J_{ij} gives the interaction between the nearest-neighbor spins (separated by \vec{r}_{ij}) and the third term represents the phonon–pseudospin interaction with the coupling constant $g_{\vec{k}s}$.

Matsushita²⁷ has extended the model of Yamada et al.²⁸ with the interaction of one phonon and one spin by considering the interactions between two spins and two phonons according to his Hamiltonian:

$$H = \frac{1}{2} \sum_{\vec{k}v} \left[p^* (\vec{k}v) p (\vec{k}v) + w_o^2 (\vec{k}v) Q^* (\vec{k}v) Q (\vec{k}v) \right] - \frac{1}{2} \sum_{\vec{q}} J_{\text{eff}} (\vec{q}) \sigma^* (\vec{q}) \sigma (\vec{q}) + \sum_{\vec{k}\vec{q}v v'} K_{1,\text{eff}} (\vec{k}\vec{q}v v') \sigma (\vec{q}) Q^* (\vec{k}v) Q (\vec{k} - \vec{q}, v') + \sum_{\vec{k}\vec{q}\vec{q}' v v'} K_{2,\text{eff}} (\vec{k}\vec{q}\vec{q}' v v') \sigma (\vec{q}) \sigma (\vec{q}') Q^* (\vec{k}v) \times Q (\vec{k} - \vec{q} - \vec{q}', v') + H_A \quad (3)$$

where

$$J_{\text{eff}} (\vec{q}) = J (\vec{q}) + \sum_v |g (\vec{q}v)|^2 \quad (4)$$

is the effective interaction parameter. In Eq. 3, the first term, in brackets, gives the interaction energy between the two phonons, and the second term is the interaction energy between the two nearest-neighbor spins. The third term describes the interaction energy between the one pseudospin and the two phonons. Finally, the fourth term is the interaction energy due to the two pseudospins and two phonons. H_A denotes the anharmonic Hamiltonian. In Eq. 3, $K_{1,\text{eff}}$ and $K_{2,\text{eff}}$ are the coefficients related to the lattice and force constants, which define the orientations of the ions (orientations of the NH_4^+ in the case of NH_4Br).

Matsushita derived the damping constant from his Hamiltonian (Eq. 3) in terms of the scattering function, and predicted the line widths of the optic modes of NH_4Br . The two models, namely, pseudospin–phonon coupled²⁹ and energy-fluctuation³⁰ models were developed from Matsushita’s Hamiltonian (Eq. 3). Those two models for the damping constant were used under the assumptions and simplifications to interpret the temperature-dependence of the line widths of the internal modes in the KDP-type materials.^{31,32} In our earlier studies, we have also applied those two models to the ammonium halides (NH_4Br and NH_4Cl)^{33,34} and $(\text{NH}_4)_2\text{SO}_4$.³⁵

Regarding the temperature-dependence of the order parameter (P), Matsushita²⁷ also derived it near T_C from MFT,²⁶ with the critical exponent $\beta = \frac{1}{2}$ according to $P \propto \left(\frac{T-T_C}{T_C}\right)^\beta$ as follows:

$$\begin{cases} \left[3\left(1 - \frac{T}{T_C}\right)\right]^{\frac{1}{2}}, & 0 < T_C - T < T_C \\ M = 1 - 2 \exp(-2T_C/T), & T \ll T_C \\ 0, & T > T_C \end{cases} \quad (5)$$

with the critical temperature, T_C , where the order parameter, P , is replaced by the magnetization, M , for the ferromagnetic materials.

CALCULATIONS AND RESULTS

The temperature-dependence of the magnetization for the MOFs, in particular, the DMNaFe compound, can also be calculated from MFT according to Eq. 5, and its critical behavior can be analyzed near T_C by means of a power-law formula:

$$M(T) = M'_0 \left(\frac{T - T_C}{T_C}\right)^\beta \quad (6)$$

where β is the critical exponent for the order parameter (magnetization) and M'_0 is the amplitude. The field-dependence of the magnetization can also be analyzed by the power-law formula:

$$M_H = M_0 \left|\frac{H - H_C}{H_C}\right|^{1/\delta} \quad (7)$$

with the critical isotherm δ and the amplitude M_0 .

The temperature-dependence of the magnetization was calculated according to Eq. 5 close to the phase transition ($T_C = 8.5$ K) for DMNaFe at 10 Oe. Our calculated $M(T)$ was then compared by fitting to the experimental magnetization measured in the ZFC and FC regimes of DMNaFe¹² according to the relationship:

$$\frac{M_{\text{cal}}}{M_0} = a + b \left(\frac{M_{\text{obs}}}{M_0}\right) + c \left(\frac{M_{\text{obs}}}{M_0}\right)^2 \quad (8)$$

with the fitted parameters a , b , and c which were determined as given in Table I. Since the magnetization increases from the low temperatures toward T_C for the ZFC regime as observed experimentally,¹²

Table I. Values of the parameters with the uncertainties by fitting M_{cal}/M_0 in the field-cooling (FC) (Eq. 5) and zero-field-cooling (ZFC) (Eq. 9) regimes to the observed data¹² for DMNaFe according to Eq. 8

DMNaFe	a	b	$-c$
FC	0.18 ± 0.02	1.82 ± 0.09	1.04 ± 0.09
ZFC	0.29 ± 0.01	1.37 ± 0.03	0.67 ± 0.03

for the calculation of $M(T)$, we employed the disorder parameter, D , defined as:

$$D = 1 - M(T) = 1 - \left[3\left(1 - \frac{T}{T_C}\right)\right]^{\frac{1}{2}} \quad (9)$$

for DMNaFe. Figure 1 gives our calculated magnetization, $M(T)$, as a function of temperature in the ferromagnetic phase ($T < T_C$) for the FC and ZFC regimes in DMNaFe.

In this part of our study, we analyzed the magnetization, $M(T)$, at various temperatures close to T_C according to the power-law formula (Eq. 6) in the log-log scale:

$$\ln M = \ln M'_0 + \beta \ln \epsilon \quad (10)$$

where the reduced temperature is $\epsilon = |T - T_C|/T_C$. From our analysis, we extracted values of the critical exponent β and the amplitude M'_0 for the FC and ZFC regimes of DMNaFe by using the experimental data.¹² Values of β and M'_0 are given in Table II and $\ln M$ as a function of $\ln \epsilon$ is plotted in Fig. 2 for both regimes (FC and ZFC) of DMNaFe.

For the analysis of $M(T)$ in the ZFC regime of DMNaFe, as it grows from the negative values to zero at $T_C = 8.5$ K,¹² we used the positive value of the magnetization ratio of M/M'_0 (Eq. 6) according to Eq. 9 with the critical exponent for the disorder parameter (D), defined as $\Delta = \beta - 1$. By writing Eq. 6 in the logarithmic form:

$$\ln\left(\frac{M}{M'_0}\right) = c_0 + \Delta \ln \epsilon \quad (11)$$

where c_0 is a constant (intercept), we determined the values of Δ and c_0 as given in Table II with the M'_0 value, as plotted in Fig. 3.

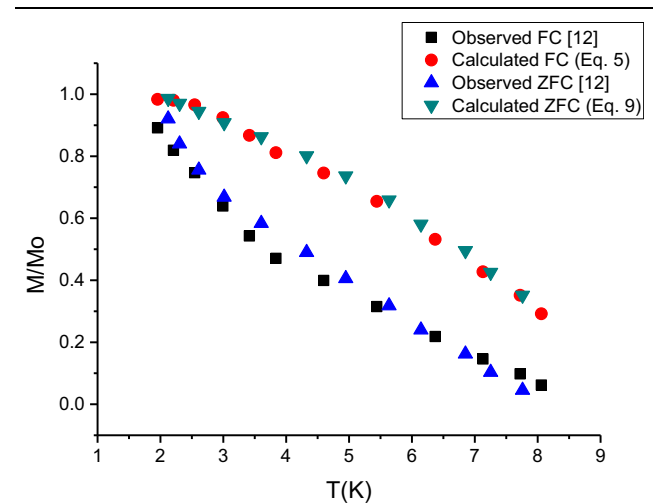


Fig. 1. Temperature variation of the magnetization M (normalized) calculated by using MFT in the field-cooling (FC) and zero-field cooling (ZFC) regimes of DMNaFe according to Eqs. (5) and (9), respectively. Magnetization data from Ref. 12 in the ZFC and FC regimes of this compound are also shown

Table II. Values of the critical exponent β for the order parameter and the amplitude M'_0 in the field-cooling (FC) regime (Eq. 10), and also values of the critical exponent Δ for the disorder parameter and the amplitude M'_0 with c_0 (Eq. 11) in the zero-field-cooling (ZFC) regime of DMNaFe ($H = 10$ Oe) within the temperature interval indicated by using the experimental data¹²

Power-law analysis	FC			ZFC			
	β	M'_0 (emu/g)	Temperature interval (K)	Δ	c_0	M'_0 (emu/g)	Temperature interval (K)
DMNaFe	0.86	59.92	$1.7 < T < 8.1$	0.32	1.27	- 116.9	$1.9 < T < 7.8$

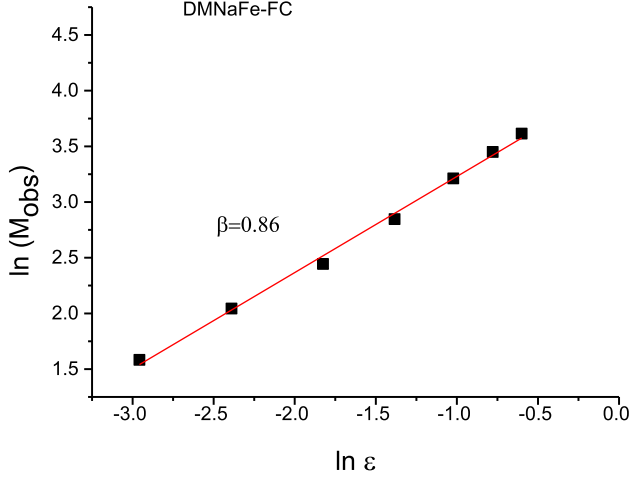


Fig. 2. Magnetization M analyzed as a function of the reduced temperature $\epsilon = |T - T_c|/T_c$ in the log-log scale with the critical temperature ($T_c = 8.5$ K) at $H = 10$ Oe according to the power-law formula with the critical exponent β for the order parameter (Eq. 10) by using the experimental data¹² in the field-cooling (FC) regime of DMNaFe

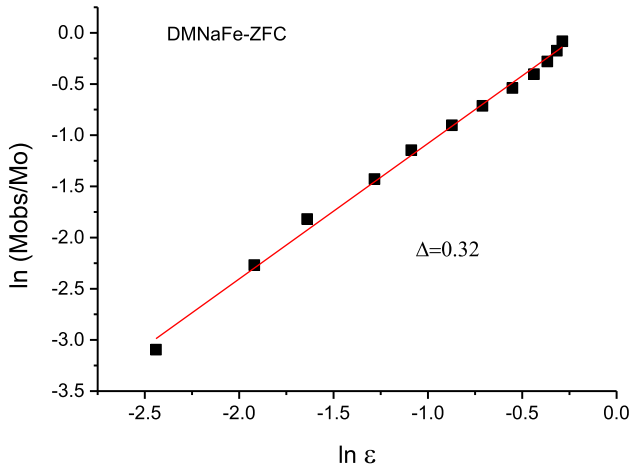


Fig. 3. Magnetization M (normalized) analyzed as a function of the reduced temperature $\epsilon = |T - T_c|/T_c$ in the log-log scale with the critical temperature ($T_c = 8.5$ K) at $H = 10$ Oe according to the power-law formula with the critical exponent Δ for the disorder parameter (Eq. 11) by using the experimental data¹² in the zero-field-cooling (ZFC) regime of DMNaFe

We also analyzed the field-dependence of the magnetization $M(H)$ according to the power-law formula (Eq. 7) in the logarithmic form:

$$\ln M_H = \ln M_0 + (1/\delta) \ln h \quad (12)$$

where $h = \frac{H-H_c}{H_c}$ is the reduced field, and we determined using the experimental data¹² the values of the critical isotherm δ (at $T_c = 8.5$ K) and M_0 , as given in Table III. $\ln M_H$ versus $\ln h$ (Eq. 12) is plotted in Fig. 4 for DMNaFe.

DISCUSSION

Magnetization $M(T)$ calculated from MFT with the critical exponent $\beta = \frac{1}{2}$ for the order parameter (Eq. 5) describes qualitatively the critical behavior of the observed magnetization,¹² which was measured as a function of temperature in the ferromagnetic phase ($T < T_c$) of DMNaFe in both the FC and the ZFC regimes, as shown in Fig. 1. Although quantitatively the observed and calculated M/M_0 do not match, they both decrease as the transition temperature ($T_c = 8.5$ K) is approached from the low temperatures for the FC and ZFC regimes in this compound. A quadratic fit (Eq. 8) was carried out to the observed $M(T)$ data¹² with the parameters a , b , and c (Table I), as shown in Fig. 1 for the FC and ZFC regimes of DMNaFe. Discrepancies between the observed and calculated $M(T)$ can be due to the inadequacy of MFT with the $\beta = \frac{1}{2}$ (Eq. 5) for the magnetization (order parameter). As $M(T)$ was calculated according to Eq. (5) on the basis of the Ising pseudospin-phonon coupled model,²⁷ the Ising model is expected to give a better description of the observed data¹² for the ferromagnetic transition in DMNaFe rather than the Heisenberg model, which provides an adequate description of antiferromagnetism and ferrimagnetism in insulating crystals as well as ferromagnetism in rare earths.²⁶ In order to describe the magnetization adequately near the T_c , the observed $M(T)$ data¹² were analyzed according to the power-law formula with the values of β for the order parameter in the FC regime (Fig. 2) and Δ for the disorder parameter in the ZFC regime (Fig. 3) with the values of β and Δ which were determined (Table II), as stated above for DMNaFe. Our value of $\beta = 0.86$ (~ 0.9) for the FC regime (Fig. 2) is too large for a second-order-type of ferromagnetic-paramagnetic transition in DMNaFe, which indicates as more likely a weakly first-order transition (nearly second-order) in this

Table III. Values of the critical isotherm δ (at $T_c = 8.5$ K) and the amplitude M_0 according to Eq. 12 within the field interval indicated for DMNaFe by using the experimental data.¹² The critical field H_c is also given

Power-law Analysis	δ	M_0	H_c (emu/g)	Field interval (emu/g)
DMNaFe	1.48	0.31	6.49	$6.49 < H < 393.39$

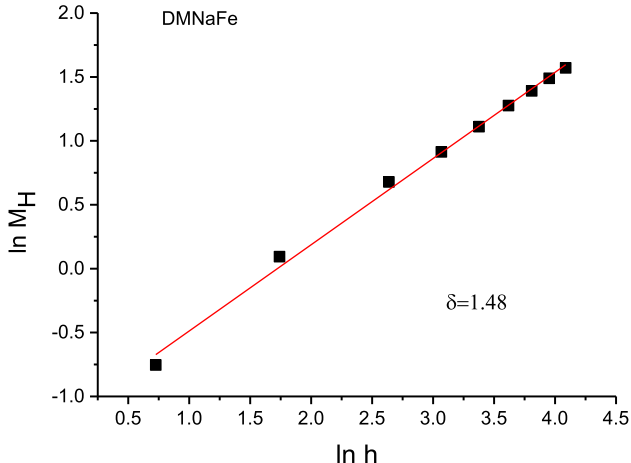


Fig. 4. Magnetization M_H analyzed as a function of the reduced magnetic field $h = \frac{H-H_c}{H_c}$ in the log-log scale with the critical field ($H_c = 6.49$ Oe) at $T_c = 8.5$ K according to the power-law formula with the critical isotherm δ (Eq. 12) by using the experimental data¹² for DMNaFe

compound. However, the value of $\Delta = 0.32$ for the disorder parameter (D) in the ZFC regime of DMNaFe is reasonable as compared to the values of $\beta(M, T) = 0.326 \pm 0.004$ and 0.38 ± 0.03 due to the three-dimensional ($d = 3$) Ising and Heisenberg ($d = 3, D = 3$) models, respectively, for a second-order ferromagnetic transition.^{36,37} On the other hand, from the analysis of the magnetization M_H as a function of the field (Eq. 7), our value of $\delta = 1.48$ for the critical isotherm (at $T_c = 8.5$ K) of DMNaFe is too small in comparison with the values of $\delta(B, M) = 3, 4.80 \pm 0.05, 4.63 \pm 0.29$ and 5 , as expected from the theoretical models of the mean field, Ising ($d = 3$), Heisenberg ($d = 3, D = 3$), and spherical ($d = 3, D = \infty$), respectively. Since all these models describe ferromagnetic-paramagnetic transition of a second-order-type in the physical systems, our M versus H analysis also indicates a weak first-order (nearly second-order) transition according to the M versus T analysis given above for the ferromagnetic transition in DMNaFe. An indication of weak first-order (nearly second-order) transition in DMNaFe is also supported by the small hysteresis visible in the magnetization, which was measured as a function of the magnetic field to describe the ferromagnetic character of the ordering in this weak ferromagnet.¹² For both the FC and ZFC regimes of DMNaFe, the $M(H)$ curve is non-linear in high magnetic fields. Below T_c , as exhibited by some metal formate frameworks (MOFs) such as DMFeCu,¹³ short-range ordering of

dimethylammonium (DMA⁺) cations can occur in DMNaFe at low temperatures, whereas, in the paramagnetic phase ($T > T_c$), the DMA⁺ cations become dynamical disorder. Also, the large negative magnetization that occurs in the ZFC regime of DMNaFe, as observed experimentally,¹² is very rare in molecular-based magnets as pointed out previously,³⁸ which was also discovered in a similar formate framework templated by DMA⁺ cations.^{39,40} The negative ZFC values were considered as due to the small negative residual field of the instrument used and the easy magnetization of the sample at $H = 10$ Oe.¹² A possibility of the occurrence of the short-range ordering of DMA⁺ cations and the negative magnetization in the ZFC regime of DMNaFe should be studied in some more detail in this compound.

CONCLUSIONS

The temperature-dependence of the magnetization, $M(T)$, was calculated in the ferromagnetic phase of DMNaFe by using MFT. It was compared with the magnetization measured as a function of temperature in the FC and the ZFC regimes as reported in the literature ($H = 10$ Oe), which we analyzed for this compound by a power-law formula. Values of the critical exponent for the order (FC) and disorder (ZFC) parameters were extracted. Analysis of the magnetization, $M(H)$, which was measured as a function of the magnetic field, was also performed by the power-law formula and the value of the critical isotherm (at $T_c = 8.5$ K) was extracted for the ferromagnetic transition in DMNaFe.

Our calculation and the analysis of the magnetization indicate that the ferromagnetic-paramagnetic transition in DMNaFe is of a weak first-order or close to a second-order. It is suggested here that calculation of the magnetization from MFT and its power-law analysis can also be performed for some other MOFs close to ferromagnetic-paramagnetic phase transitions.

CONFLICT OF INTEREST

The authors declare that they have no conflict of interest.

REFERENCES

1. P. Jain, V. Ramachandran, R.J. Clark, H.D. Zhou, B.H. Toby, N.S. Dalal, H.W. Kroto, and A.K. Cheetham, *J. Am. Chem. Soc.* 131, 13625 (2009).
2. L.E. Kreno, K. Leong, O.K. Farha, M. Allendorf, R.P. Van Duyne, and J.T. Hupp, *Chem. Rev.* 112, 1105 (2012).
3. M. Maczka, A. Ciupa, A. Gagor, A. Sieradzki, A. Pikul, B. Macalik, and M. Drozd, *Inorg. Chem.* 53, 5260 (2014).

4. K. Szymborska-Malek, M. Trzebiatowska-Gutowska, M. Maczka, and A. Gagor, *Spectrochimica Acta A* 159, 35 (2016).
5. J.Y. Lee, O.K. Farha, J. Roberts, A.K. Scheidt, S.T. Nguyen, and J.T. Hupp, *Chem. Soc. Rev.* 38, 1450 (2009).
6. M.D. Allendorf, C.A. Bauer, R.K. Bhakta, and R.J.T. Houk, *Chem. Soc. Rev.* 38, 1330 (2009).
7. G. Rogez, N. Viart, and M. Drillon, *Angew. Chem. Int. Ed.* 49, 1921 (2010).
8. W. Zhang and R.G. Xiong, *Chem. Rev.* 112, 1163 (2012).
9. J.A. Mason, M. Veenstra, and J.R. Long, *Chem. Sci.* 5, 32 (2014).
10. A. Rossin, G. Giambastiani, M. Peruzzini, and R. Sessoli, *Inorg. Chem.* 51, 6962 (2012).
11. M. Maczka, B. Bondzior, P. Dereń, A. Sieradzki, J. Trzmiel, A. Pietraszko, and J. Hanuza, *Dalton Trans.* 44, 6871 (2015).
12. M. Maczka, A. Pietraszko, L. Macalik, A. Sieradzki, J. Trzmiel, and A. Pikul, *Dalton Trans.* 43, 17075 (2014).
13. A. Ciupa, M. Maczka, A. Gagor, A. Pikul, and M. Ptak, *Dalton Trans.* 44, 13234 (2015).
14. M. Maczka, M. Ptak, K. Hermanowicz, A. Majchrowski, A. Pikul, and J. Hanuza, *Phys. Rev. B* 83, 174439 (2011).
15. M. Fiebig, *J. Phys. D* 38, R123 (2005).
16. Y. Tokura, *J. Magn. Magn. Mater.* 310, 1145 (2007).
17. M. Maczka, A. Gagor, B. Macalik, A. Pikul, M. Ptak, and J. Hanuza, *Inorg. Chem.* 53, 457 (2014).
18. X.Y. Wang, L. Gan, S.W. Zhang, and S. Gao, *Inorg. Chem.* 43, 4615 (2004).
19. P. Jain, N.S. Dalal, B.H. Toby, H.W. Kroto, and A.K. Cheetham, *J. Am. Chem. Soc.* 130, 10450 (2008).
20. M. Sanchez-Andujar, S. Presedo, S. Yanez-Vilar, S. Castro-Garcia, J. Shamir, and M.A. Senaris-Rodriguez, *Inorg. Chem.* 49, 1510 (2010).
21. G.C. Xu, W. Zhang, X.M. Ma, Y.H. Hen, L. Zhang, H.L. Cai, Z.M. Wang, R.G. Xiong, and S. Gao, *J. Am. Chem. Soc.* 133, 14948 (2011).
22. P. Pato-Dolan, L.C. Gomez-Aguirre, J.M. Bermudez-Garcia, M. Sanchez-Andujar, A. Fondado, J. Mira, S. Castro-Garcia, and M.A. Senaris-Rodriguez, *RSC Adv.* 3, 22404 (2013).
23. H. Yurtseven and E.K. Dogan, *Polyhedron* 154, 132 (2018).
24. E.K. Dogan and H. Yurtseven, *Curr. Appl. Phys.* 19, 1096 (2019).
25. H. Yurtseven and E.K. Dogan, *Mater. Res. Bull.* 119, 110572 (2019).
26. R. Brout, *Phase Transitions* (New York: Benjamin, 1965) Ch 2.
27. M. Matsushita, *J. Chem. Phys.* 65, 23 (1976).
28. Y. Yamada, M. Mori, and Y. Noda, *J. Phys. Soc. Jap.* 32, 1565 (1972).
29. G. Lahajnar, R. Blinc, and S. Zumer, *Phys. Condens. Matter* 18, 301 (1974).
30. G. Schaack and V. Winterfeldt, *Ferroelectrics* 15, 35 (1977).
31. I. Laulicht and N. Luknar, *Chem. Phys. Lett.* 47, 237 (1977).
32. I. Laulicht, *J. Phys. Chem. Solids* 39, 901 (1978).
33. H. Yurtseven, *Spectrochim. Acta A* 62, 910 (2005).
34. H. Yurtseven and H. Karacali, *Spectrochim. Acta A* 65, 421 (2006).
35. H. Yurtseven, H. Karacali, and A. Kiraci, *Int. J. Mod. Phys. B* 25, 2063 (2011).
36. H.E. Stanley, *Introduction to Phase Transitions and Critical Phenomena* (Oxford: Clarendon, 1971) Ch 3.
37. J.J. Binner, N.J. Dowrick, A.J. Fisher, and M.E.J. Newman, *The Theory of Critical Phenomena: An Introduction to the Renormalization Group* (New York: Oxford University Press, 1992) Chapter 3.
38. J.P. Zhao, B.W. Hu, F. Lioret, J. Tao, Q. Yang, X.F. Zhang, and X.H. Bu, *Inorg. Chem.* 49, 10390 (2010).
39. L. Canadillas-Delgado, O. Fabelo, J.A. Rodriguez-Velamazán, M.H. Lemee-Cailleau, S.A. Mason, E. Pardo, F. Lloret, J.P. Zhao, X.H. Bu, V. Simonet, C.V. Colin, and J. Rodriguez-Carvajal, *J. Am. Chem. Soc.* 134, 19772 (2012).
40. M. Maczka, A. Ciupa, A. Gagor, A. Sieradzki, A. Pikul, and M. Ptak, *J. Mater. Chem.* 4, 1186 (2016).

Publisher's Note Springer Nature remains neutral with regard to jurisdictional claims in published maps and institutional affiliations.